Primary, seminal and lateral roots of maize show type-specific growth and hydraulic responses to water deficit

Virginia Protto, Fabrice Bauget, Louai Rishmawi, Philippe Nacry, Christophe Maurel

https://doi.org/10.1093/plphys/kiad675 PLANT PHYSIOLOGY 2024: 00: 1–16

Plant Physiology®

Research Article

Primary, seminal and lateral roots of maize show type-specific growth and hydraulic responses to water deficit

Virginia Protto, Fabrice Bauget, Louai Rishmawi, Philippe Nacry and Christophe Maurel*

Institute for Plant Sciences of Montpellier (IPSiM), Univ Montpellier, CNRS, INRAE, Institut Agro, 2 place Viala, 34060 Montpellier, France

*Author for correspondence: christophe.maurel@cnrs.fr
The author responsible for distribution of materials integral to the findings presented in this article in accordance with the policy described in the Instructions for Authors (https://academic.oup.com/plphys/pages/General-Instructions) is Christophe Maurel.

Abstract

The water uptake capacity of a root system is determined by its architecture and hydraulic properties, which together shape the root hydraulic architecture. Here, we investigated root responses to water deficit (WD) in seedlings of a maize (*Zea mays*) hybrid line (B73H) grown in hydroponic conditions, taking into account the primary root (PR), the seminal roots (SR), and their respective lateral roots. WD was induced by various polyethylene glycol concentrations and resulted in dose-dependent inhibitions of axial and lateral root growth, lateral root formation, and hydraulic conductivity (Lp_r), with slightly distinct sensitivities to WD between PR and SR. Inhibition of Lp_r by WD showed a half-time of 5 to 6 min and was fully (SR) or partially (PR) reversible within 40 min. In the two root types, WD resulted in reduced aquaporin expression and activity, as monitored by mRNA abundance of 13 plasma membrane intrinsic protein (ZmPIP) isoforms and inhibition of Lp_r by sodium azide, respectively. An enhanced suberization/lignification of the epi- and exodermis was observed under WD in axial roots and in lateral roots of the PR but not in those of SR. Inverse modeling revealed a steep increase in axial conductance in root tips of PR and SR grown under WD that may be due to the decreased growth rate of axial roots in these conditions. Overall, our work reveals that these root types show quantitative differences in their anatomical, architectural, and hydraulic responses to WD, in terms of sensitivity, amplitude and reversibility. This distinct functionalization may contribute to integrative acclimation responses of whole root systems to soil WD.

Introduction

Water is fundamental for plant life contributing to key biochemical processes such as photosynthesis, acting as a carrier of metabolites and nutrients, and mediating structural support through turgor pressure. In the soil–plant–atmosphere continuum, water always moves toward lowest water potentials. In well-watered conditions, water can readily be absorbed by the plant to sustain growth and transpiration (Jackson et al. 2000; Steudle 2001). Under drought, however, as the soil water potential decreases, plants need to implement specific strategies to sustain water acquisition and maintain their water status.

The key role played by roots in water acquisition can easily be grasped in relation to their highly specialized anatomy and architecture (McCully and Canny 1988; Lynch et al. 2014). Continuous growth and branching of plant roots results in a complex network defined as root system architecture (RSA) (Lynch 1995; Maurel and Nacry 2020). Multiple parameters of RSA such as the length (depth) of the main root(s), the density and elongation of lower-order roots, their gravitropic set-point angle and the possible presence of adventitious roots or crown roots (Maurel and Nacry 2020) contribute to the capacity of roots to forage for water under varying soil conditions. Conversely, numerous environmental

Received August 23, 2023. Accepted November 27, 2023. Advance access publication January 13, 2024

factors govern the growth and development of roots thereby shaping their highly specialized adaptive responses to abiotic and biotic constraints (McCully 1999; Hochholdinger et al. 2004b; Zhan et al. 2015; Gao and Lynch 2016).

Like other cereals, maize (*Zea mays* L.) has a complex RSA composed of embryonic and postembryonic axial root types. The former comprise a primary root (PR) and several seminal roots (SR) which contribute to the early vigour and establishment of the seedling; postembryonic roots include lateral roots (LR) and shoot-born crown roots (CR) and brace roots (BR) (Hochholdinger et al. 2004a). Maize mutants exhibiting specific root alterations have revealed that each root type develops according to an endogenous genetic program (Bray and Topp 2018; Hochholdinger et al. 2018). In addition, anatomical studies in the maize inbred line B73 have shown that, with respect to PR and CR, SR exhibit unique anatomic traits such as smaller total area and stele area, and reduced number of cortical cells (Tai et al. 2016). Inspection of a larger panel of inbred lines confirmed these observations and revealed, in some genotypes, a distinct xylem anatomy between PR and SR (Rishmawi et al. 2023). In addition, SR were found to exhibit a distinct transcriptome with an abundance of stress-related genes and transcription factors, while the predominant functions revealed in PR and CR transcriptomes were associated with cell wall formation and cell remodeling (Tai et al. 2016). Despite their differences, all axial root types carry LR which supposedly mediate most of the nutrient and water uptake (Lynch 1995).

Upon entry into the root, water is first transported radially to the stele along cell walls (apoplastic pathway) or from cell-to-cell, across the symplasm (through plasmodesmata) or across cell membranes, mostly through aquaporins (AQP). Water is then loaded into the xylem and transported to the leaves. Furthermore, depending on the plant's developmental stage, the different root types may achieve distinct roles in water uptake (Hochholdinger and Tuberosa 2009; Ahmed et al. 2016, 2018). In maize seedlings for instance, LR are believed to be primarily responsible for the majority of water absorption from the soil. Conversely, the PR and SR axially transport the water collected by LR to the shoot (Ahmed et al. 2016). During the later stages of maize plant development, CR, in conjunction with LR, seem to exhibit the highest water transport capacity (Ahmed et al. 2018). In most plant species, water deficit (WD) induces deep modifications of root hydraulics (root hydraulic conductivity: Lp_r) by an early regulation of AQP function and, at later stages, by alterations of root cell suberization and xylem differentiation (Vandeleur et al. 2009; Hachez et al. 2012; Ramachandran et al. 2018). Notably, it was observed in different plants including Arabidopsis (*Arabidopsis thaliana*) and maize that a mild WD stimulates Lp_r to possibly optimize water uptake (Siemens and Zwiazek 2004; Sutka et al. 2011; Hachez et al. 2012; Dowd et al. 2019; Rosales et al. 2019). On the contrary, severe WD dramatically inhibited Lp_r thereby reducing the exchanges between the root and its environment (Sharp and Davies 1989; Schmidhalter et al. 1998; Siemens and Zwiazek 2004; Rosales et al. 2019). Thus, a comprehensive understanding, in each root type, of links between root hydraulics, anatomy and WD intensity is critically needed.

The availability of soil water also profoundly shapes RSA (Steudle 2000; Maurel et al. 2015; Tang et al. 2018). Under mild WD, most plant species develop a deeper root system to promote water acquisition (Sharp and Davies 1985; Schmidhalter et al. 1998; Dowd et al. 2019; Rosales et al. 2019) whereas others may promote the growth of shallow roots in anticipation of episodic showers (Ogura et al. 2019). Severe WD generally exert inhibitory effects on root growth, although some root types, such as maize PR and nodal roots, sustain their elongation thereby foraging for water in deeper layers of the soil (Sharp and Davies 1979; Sharp et al. 1988, 2004; Van der Weele et al. 2000). LR formation and growth also show strong and specific responses to soil water content (Seiler 1998). In maize, for example, the formation and elongation of LR on the PR (LR_{prim}) showed dose-dependent responses to WD that were either bell-shaped or monotonous, depending on genotypes (Dowd et al. 2019). In natural or field conditions, most of these growth phenomena occur concomitantly during the course of root growth and water acquisition, allowing plant roots to integrate complex changes in space and time of soil water availability. Thus, dissecting effects of well-controlled WD on specific root types may help deciphering the complexity of these processes.

The water uptake capacity of a root system is determined by both its architecture and hydraulic properties, which together shape the root hydraulic architecture (Maurel and Nacry 2020; Rishmawi et al. 2023). In a recent study aimed at elucidating the water uptake capacity of maize seedlings, the root hydraulic architecture of plants grown under standard conditions was analyzed in a panel of 224 inbred Dent lines (Rishmawi et al. 2023). Although comparable hydraulics were found in PR and SR of a given genotype, this study revealed dramatic differences in RSA and hydraulics between genotypes. A functional–structural model of root systems further showed substantial genotypic differences in xylem conductance profile and emphasized the broad range of water uptake strategies present in the diversity panel (Rishmawi et al. 2023). Except for a recent study on Arabidopsis (Rosales et al. 2019), which pointed to the coordinating role of abscisic acid (ABA), there have been few works addressing the integration of hydraulic and growth responses of roots to WD. In the present work, we performed such analysis focusing on maize hybrid line (B73H) seedlings with two main aims: (i) to address the integration and consistency of architectural, anatomical, and hydraulic responses to WD, (ii) to understand the precise functions of different root types, taking into account the PR, SR, and their respective LR (LR_{prim}, LR_{sem}). Our work reveals that these root types show quantitative differences in their responses to WD, in terms of sensitivity, amplitude, and reversibility. Differences in anatomical and molecular responses may support this distinct root functionalization and contribute to integrative acclimation responses of root systems to WD.

Results

Dose-dependent response of RSA to WD

In order to analyse the architectural response of PR and SR to different WD intensities, maize plants were hydroponically grown under control conditions until 11 days after sowing (DAS) or, from 7 to 11 DAS, in the presence of various concentrations (25 to 225 g L^{-1}) of a high molecular weight polyethylene glycol (PEG-8000) yielding final external water potentials from −0.034 MPa (Control) to −0.7 MPa (225 g L^{-1} PEG; 225PEG) (Supplementary Fig. S1). The latter water potential corresponds to a rather severe drought condition in maize (Caldeira et al. 2014; Koehler et al. 2023). Measurements were refined in roots treated for 4 d with 50 g L^{-1} PEG (50PEG; −0.070 MPa) or 150 g L^{-1} PEG (150PEG; −0.332 MPa) (Fig. 1A), which mimics

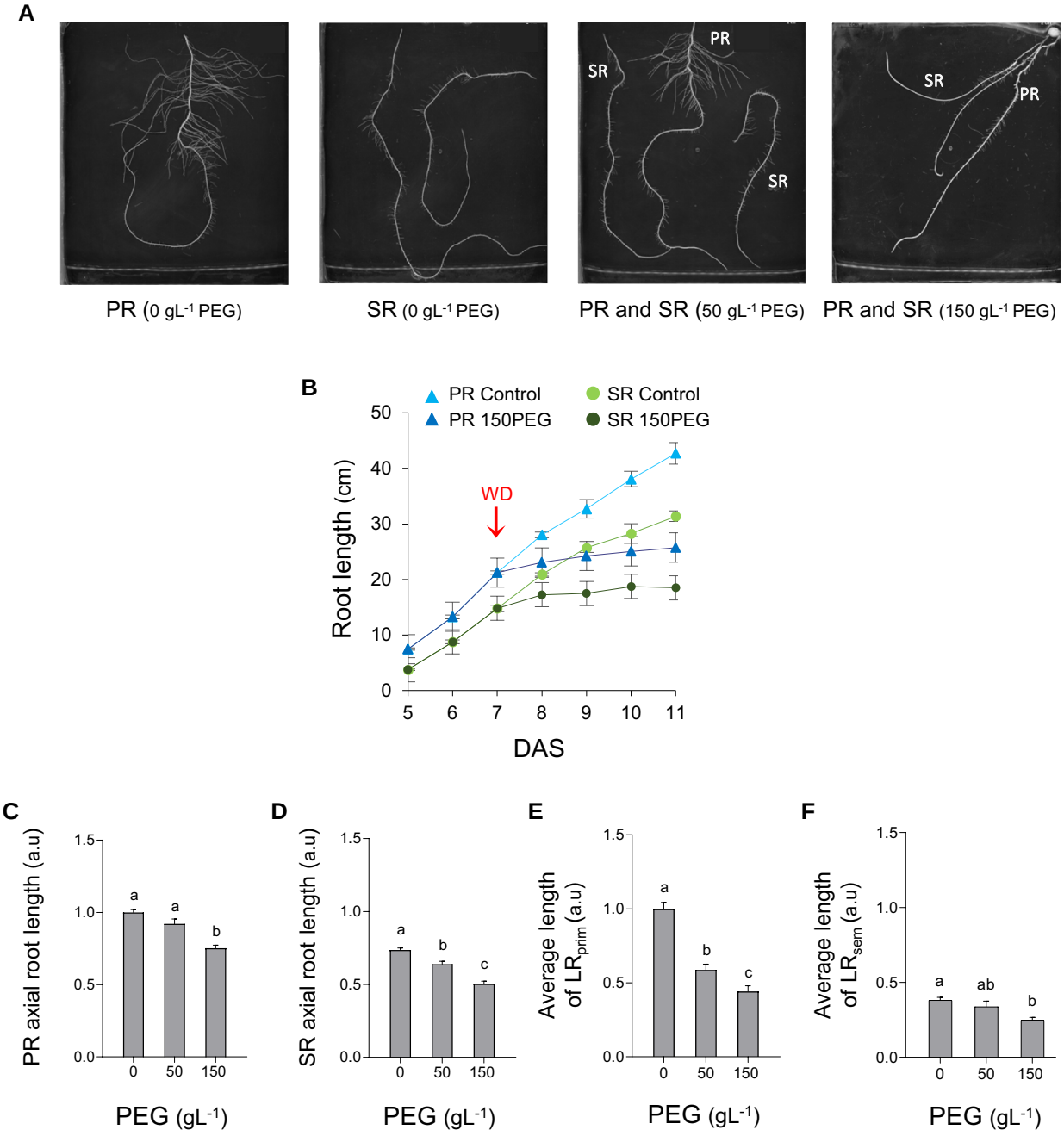

Figure 1. RSA response of PR and SR to PEG-induced WD. **A)** Representative images of PR or SR of plants exposed to the indicated PEG concentration for 4 d. **B)** Growth kinetics of PR (blue triangles) and SR (green circles) in control (light blue, light green) or 150PEG (dark blue, dark green) conditions. Red arrow indicates the time of PEG application (cumulated data from two independent plant cultures; PR: $n = 38$, SR: $n = 48$). **C to F)** Axial length of PR (**C**), axial length of SR (**D**), LR_{prim} length (**E**), and LR_{sem} length (**F**) after 4 d in the presence of the indicated PEG concentration. Data in (**C**) and (**D**) are normalized to PR length in control conditions while data in (**E**) and (**F**) are normalized to LR_{prim} length in control conditions. For (**C**) to (**F**), the figure shows cumulated data from seven independent experiments (PR: $n = 35$ to 75; SR: $n = 50$ to 120). Error bars indicate SEM. For each root type, different letters indicate statistically different values (ANOVA followed by Tukey test; $P < 0.05$).

a moderate WD (Caldeira et al. 2014). All growth and developmental parameters measured in the PR and SR and their laterals are shown in Fig. 1 and Supplementary Figs. S1 and S2. Here, we examined in particular the growth rate of axial roots and the length of their LR in plants grown under 50PEG and 150PEG conditions (Fig. 1, B to F). Over the full hydroponic growth period (from 5 to 11 DAS), PR and SR grew in control conditions by 5.1 ± 0.3 and 3.9 ± 0.3 cm d^{-1}, respectively. Under 150PEG conditions, PR and SR reduced their growth rate to 0.8 ± 0.2 and 0.5 ± 0.1 cm d^{-1}, respectively (Fig. 1B). Thus, PR showed a higher growth rate than SR during the whole course of our experiments, by $34 \pm 5\%$ and $50 \pm 4\%$, under control and 150PEG conditions, respectively (Fig. 1B). Overall, exposure to 150PEG resulted in a reduction in axial root length (at 11 DAS) by 25% and 39% for PR and SR, respectively (Fig. 1, C and D). By comparison, a 50PEG treatment had no significant effect on PR length while it caused a reduction in SR length by 12% (Fig. 1, C and D).

Concerning LR, the average length of LR_{prim} was reduced by 41% and 56%, under 50PEG and 150PEG conditions as compared to that under control conditions, respectively. By comparison, LR_{sem} were notably smaller than LR_{prim} since they were mostly formed during the last 4 d of culture, i.e. during the WD treatment. Yet, the average length of LR_{sem} was not altered under 50PEG conditions, as compared to that under control conditions, while being reduced by 34% under 150PEG conditions (Fig. 1, D to E). The overall data (Fig. 1; Supplementary Figs. S1 and S2) indicate that axial growth rate of SR is lower and more sensitive to WD than that of PR. In contrast, PR are more sensitive than SR regarding LR growth.

Dose- and AQP-dependent response of root hydraulics to WD

We next explored the dose-dependent impact of WD on the root hydraulic properties of maize seedlings using the pressure chamber technique. The conductance and balancing pressure (see Supplementary Fig. S3), and resulting Lp_r values were measured on individual PR and SR excised from plants grown in the absence or presence of PEG. In control conditions, PR showed a mean Lp_r of 75 ± 4.8 mL h^{-1} MPa^{-1} g^{-1}, which was 31% higher than that of SR ($Lp_r = 52 \pm 3.3$ mL h^{-1} MPa^{-1} g^{-1}) (Fig. 2, A and B). A 50PEG treatment had no significant effect on Lp_r of PR while it reduced the Lp_r of SR by 47%. In contrast, exposure to 150PEG led to a Lp_r reduction by 87% in PR and 79% in SR. Thus, SR appear to be more sensitive than PR regarding Lp_r inhibition by WD (Fig. 2, A and B).

Water uptake by plant roots can be mediated by AQP (Javot and Maurel 2002; Maurel et al. 2015). To evaluate AQP contribution to Lp_r under control and 150PEG conditions, we applied 1 mM sodium azide, a well-characterized AQP blocker (Sutka et al. 2011; Rishmawi et al. 2023), and measured the residual Lp_r. Under control conditions, azide treatment resulted in a 58% reduction of Lp_r (Fig. 3A) in both PR and SR. Azide exerted a lower but significant inhibitory effect (−33%) on the Lp_r of PR under 150PEG treatment

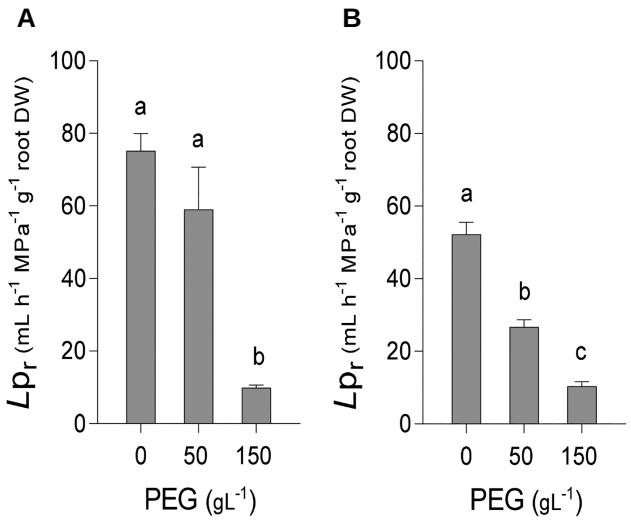

Figure 2. Root hydraulic response of PR and SR to WD. Lp_r of individual PR (**A**) or SR (**B**) excised from plants grown for 4 d in the presence of the indicated PEG concentration. Cumulated data from eight independent plant cultures for 0 and 150 g L^{-1} PEG (PR: $n = 76$ to 82; SR: $n = 54$ to 67) and three independent plant cultures for 50 g L^{-1} PEG (PR: $n = 20$; SR: $n = 15$). Error bars indicate SEM. For each root type, different letters indicate statistically different values (ANOVA followed by Tukey test; $P < 0.05$).

whereas it had no effect on the Lp_r of SR under the same treatment (Fig. 3B). The data indicate that AQP contribute in large part to the Lp_r of PR and SR under control conditions. Their inhibition can account at least partially for the effects of WD on Lp_r. Furthermore, azide-sensitive AQP are totally inhibited after 150PEG in SR while they remain partially active in PR.

Dynamics of Lp_r modulation in PR and SR

To investigate the dynamics of PR and SR hydraulics under WD, we monitored short-time variations of Lp_r following changes in root bathing conditions. When roots of 11-d-old plants grown under control conditions were transferred to a 150PEG solution, the Lp_r of both PR and SR rapidly decreased, with a half-time ($t_{1/2}$) of 5 to 6 min (Fig. 4, A and B), down to values similar to those observed in plants of the same age, but treated for 4 d with a similar PEG concentration. Comparable variations in Lp_r were observed using bathing solutions that contained osmotically equivalent sorbitol concentrations (Supplementary Fig. S4). In the converse experiments, PR and SR of 11-d-old plants that had been grown for 4 d under 150PEG conditions and were shifted to a control condition showed a rapid increase of their Lp_r, with $t_{1/2}$ of 11 to 19 min (Fig. 4, A and B). In these experiments, Lp_r of PR was partially restored, to 59% of its control value, whereas Lp_r of SR showed a complete reversion, to 107.5% of its control values (Fig. 4, A and B). We conclude that both PR and SR show a rapid inhibition of Lp_r in response to WD, which is partially (PR) or fully (SR) reversible over a short time (<1 h).

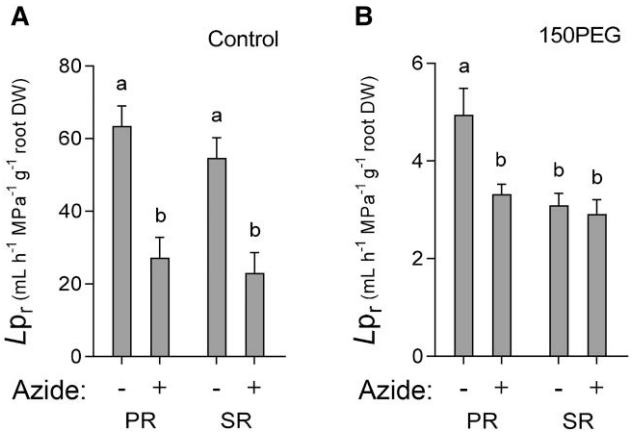

Figure 3. Effects of azide on root hydraulics. Lp_r of PR and SR of plants grown in control conditions (**A**) or after 4 d of a 150PEG treatment (**B**), and measured in the absence (−) or presence (+) of 1 mM sodium azide. Cumulated data from two independent plant cultures (PR: $n = 18$ to 28; SR: $n = 16$ to 26). Error bars indicate SEM. For each root type, different letters indicate statistically different values (ANOVA followed by Tukey test; $P < 0.05$).

ZmPIP1 and *ZmPIP2* gene expression in PR and SR after short- and long-term WD

To address the molecular bases of distinct hydraulic properties of PR vs. SR, we used reverse transcription quantitative PCR (RT-qPCR) and monitored the expression of six *PLASMA MEMBRANE INTRINSIC PROTEIN 1* (*ZmPIP1*) and seven *ZmPIP2* genes. For both PR and SR, a distinction was made between the LR and the unbranched part of the axial root. Figure 5 shows data for the most highly expressed *PIP*s (*ZmPIP1;1*, *ZmPIP1;5*, *ZmPIP2;1*, *ZmPIP2;5*, *ZmPIP2;6*). For plants grown in control conditions, the expression level of genes, such as *ZmPIP1;1*, *ZmPIP2;5* and *ZmPIP2;6* was >2-fold higher in LR_{prim} than in LR_{sem} (Fig. 5A). A 4 d exposure to 150PEG induced in LR_{prim} a reduction of *ZmPIP* expression compared to that under control conditions, which was greater than 2-fold in the case of *ZmPIP1;1* and *ZmPIP2;6* (Fig. 5A), whereas WD had no effect on *ZmPIP* expression in the LR_{sem} (Fig. 5A). Under control conditions, *ZmPIP* mRNA abundance was similar in the unbranched parts of PR and SR (Fig. 5B). Furthermore, exposure for 4 d to 150PEG resulted in a significant reduction in abundance of *ZmPIP2;1* and *ZmPIP2;6* mRNA and of *ZmPIP2;1* mRNA, in the unbranched parts of PR and SR, respectively, compared with that under control conditions. In both root types, all other *ZmPIP* mRNAs showed a similar tendency to lower abundance under 150PEG conditions compared with under control conditions (Fig. 5B). The overall data indicate that in control conditions *ZmPIP* genes are more highly expressed in LR_{prim} than in LR_{sem} and a long-term WD induces a reduction of *ZmPIP* expression in the former but not the latter root types (Fig. 5A). By contrast, the axial root tips of PR and SR show similar *ZmPIP* expression profiles and similar reduction in *ZmPIP* expression under WD (Fig. 5B).

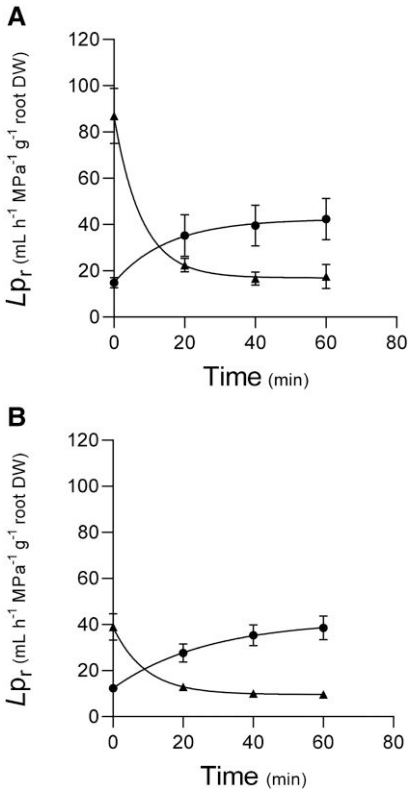

Figure 4. Kinetic analysis of Lp_r in PR and SR in response to a sudden change in PEG concentration in the bathing solution. Plants grown in control (triangle) or 150PEG (circles) conditions for 4 d were transferred at time = 0 to a 150PEG or control solution, respectively. Lp_r of PR (**A**) or SR (**B**) was measured at the indicated time after transfer. Cumulated data from five independent plant cultures for PR ($n = 16$ to 24), and three independent plant cultures for SR ($n = 15$). Error bars indicate SE. The experimental data were fitted using a one-phase decay exponential function.

To better understand the kinetic effects of water availability on Lp_r (Fig. 4), we investigated the effects of the same treatments on *ZmPIP* expression, considering the whole set of six *ZmPIP1* and seven *ZmPIP2* genes. As described above, hydroponically grown plants were shifted from a control to a 150PEG solution, and vice versa, and root tissues were collected after 1 h (Fig. 6). Here, we focused on the response of the axial unbranched parts of PR and SR, while essentially similar results obtained in LR are shown in Supplementary Fig. S5. In PR, the transfer to 150PEG resulted in a rapid reduction (between 43% and 65%) of the relative gene expression of *ZmPIP1;1*, *ZmPIP2;1* and *ZmPIP2;5* and a comparable, although not significant, response for *ZmPIP1;5* and *ZmPIP2;6* (Fig. 6A). A similar trend was observed in the unbranched parts of SR (Fig. 6B). In converse experiments, root transfer from a 150PEG to a control solution did not induce any change in *ZmPIP* gene expression, except for an increase in mRNA abundance of *ZmPIP1;1* in PR (Fig. 6A) and of *ZmPIP1;5* in SR (Fig. 6B). Therefore, WD induces a reduction in *ZmPIP* gene expression in PR and SR that somewhat

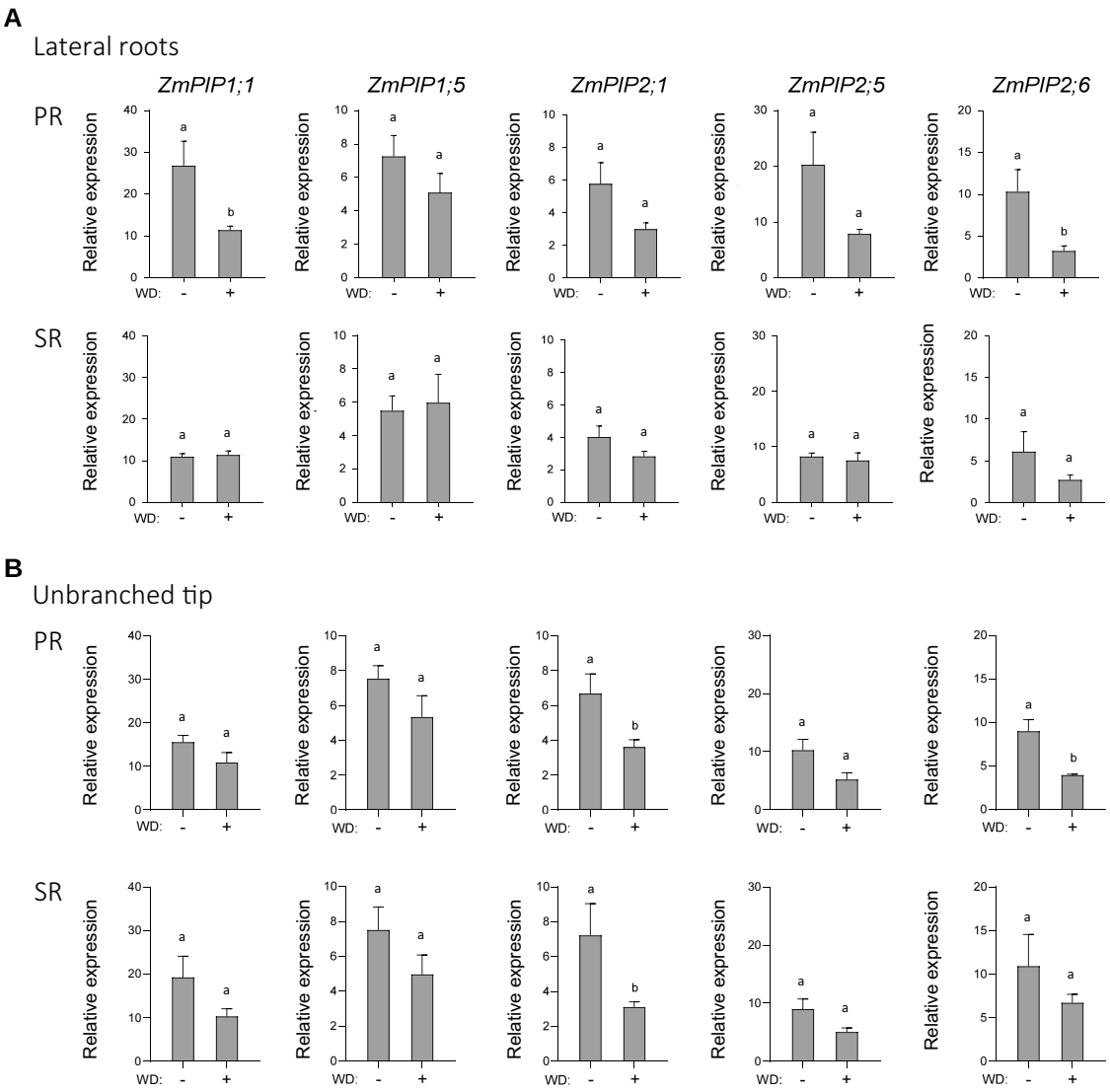

Figure 5. Effects of a 4-d-long 150PEG treatment on relative expression of selected *ZmPIP1* and *ZmPIP2* genes. mRNA abundance of the most highly expressed *ZmPIP1* (*ZmPIP1;1*, *ZmPIP1;5*) and *ZmPIP2* (*ZmPIP2;1*, *ZmPIP2;5*, *ZmPIP2;6*) genes in LR (**A**) and in the unbranched zone (**B**) of PR and SR. mRNA abundance was monitored under control conditions (WD: −) or after 4 d of a 150PEG treatment (WD: +). Cumulated data from three independent biological repeats (each with four segments from four independent roots for each zone). Error bars indicate SEM. For each root type, different letters indicate statistically different values (Unpaired *t* test; $P < 0.05$).

accompanies a decrease in their Lp_r. By contrast, shifting of both root types from WD to control conditions does not alter *ZmPIP* gene expression whereas a recovery of Lp_r can be observed.

Root anatomy and its response to WD

To gain a deeper understanding of the impact of WD on both axial and radial water transport, and thereby on Lp_r, we performed a thorough anatomical analysis of PR and SR and their LR. For this, we used plants that had been subjected for 4 d to a 150PEG treatment, and investigated in both PR and SR three specific segments (I to III), that were defined according to their time of formation during WD exposure (Fig. 7A). Taking into account differences in growth rate between roots in control and WD conditions, segment III corresponds to the most basal and early (6 DAS) segment and serves as a control. By contrast, segments II and I are closer to the root tip, and were formed after 1 or 3 d of treatment, at 8 and 10 DAS, respectively. LR_{prim} and LR_{sem} were sampled in segments III and sectioned in regions formed after WD application.

Suberin and lignin deposition in the epi-, exo-, and endodermis (Fig. 7B) can be enhanced under WD, thereby altering radial hydraulic conductivity (Calvo-Polanco et al. 2021; Shukla and Barberon 2021). Here, we found that, in segments III of both PR and SR, a 150PEG treatment had the tendency to increase suberin/lignin deposition in all three cell types (Fig. 7, C and D; Supplementary Fig. S6). We also detected a similar response in segments I, in particular in the PR endodermis (Fig. 7C; Supplementary Fig. S6). LR_{prim} under 150PEG

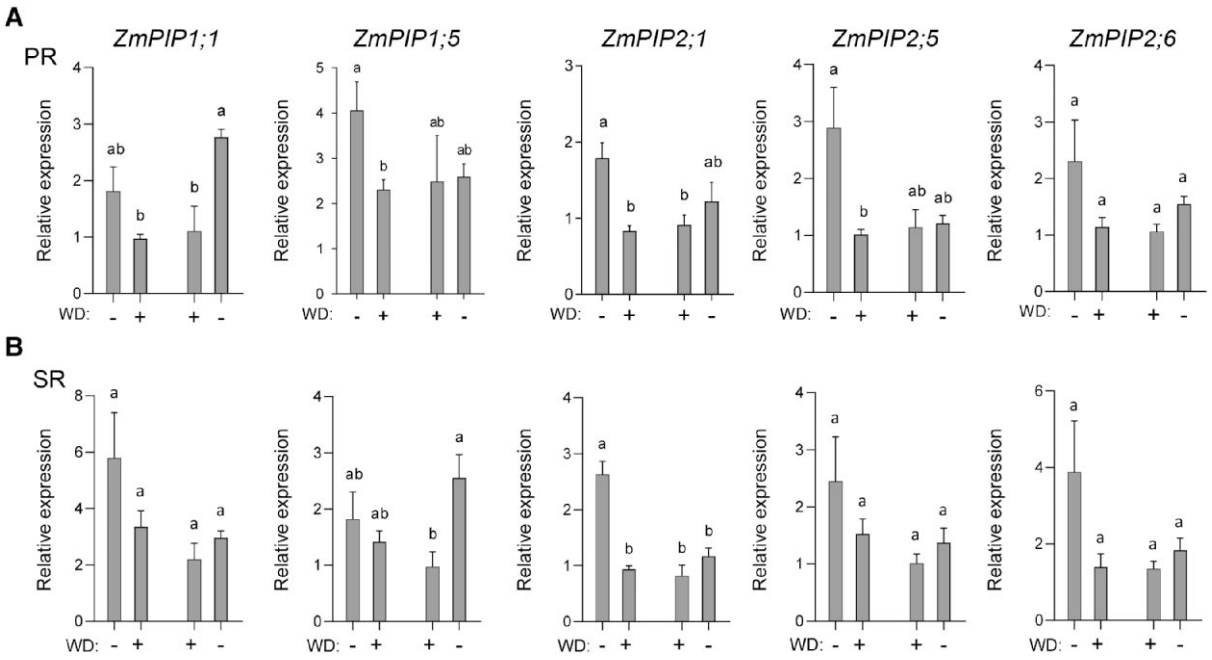

Figure 6. Relative expression of selected *ZmPIP1* and *ZmPIP2* genes in the unbranched zone of PR and SR after short-term (1 h) change in PEG concentration in the root bathing solution. The figure shows the relative mRNA abundance of the indicated *ZmPIP* in PR (**A**) and SR (**B**). The left-hand side of each panel shows *PIP* expression in roots of 11-d-old plants grown in hydroponic control conditions during the last 4 d (WD: −) and shifted to a 150PEG solution for 1 h (WD: +). Conversely, the right-hand side of each panel shows *PIP* relative expression in roots of plants of the same age but grown in a 150PEG solution during the last 4 d (WD: +) and shifted to a control solution (WD: −) for 1 h. Cumulated data from two independent biological repeats (each with four segments from four independent roots). Error bars indicate SEM. For each root type, different letters indicate statistically different values (Unpaired *t* test; $P < 0.05$).

conditions also showed a significant increase in suberin/lignin deposition in both exodermis and epidermis, and a similar tendency in endodermis. By contrast, suberization/lignification of LR_{sem} was not altered by WD (Fig. 8, A to F).

Root diameter and thickness of the cortex were also analyzed in segments I to III of PR and SR (Supplementary Fig. S7). In control conditions, these two traits diminished from PR base to tip whereas they remained constant in SR. Under 150PEG conditions, the two traits remained similar along PR length or even increased in the newly formed SR parts (segment I) (Supplementary Fig. S7). Thus, WD induced a thickening of the PR and SR tips. Finally, WD induced in both LR_{prim} and LR_{sem} an increase in cross section diameter and a thickening of root cortex (Supplementary Fig. S8).

Xylem anatomy was also inspected to possibly get insights into the axial conductance of PR and SR under control and WD conditions. The total area and number of early and late metaxylem vessels were higher in the PR than in the SR (Supplementary Fig. S7). However, a 4 d 150PEG treatment had no significant impact on either of these parameters, except for an increase in late metaxylem area in apical segments (I) of PR.

In summary, a 4 d WD treatment had no marked effect on the anatomy of the vascular tissues. In contrast, it induced a thickening of the PR and SR tips and of LR_{prim} and LR_{sem}. A similar response was previously reported in wheat (*Triticum aestivum*) (Ji et al. 2014). The WD treatment also increased suberization/lignification in PR, SR, and LR_{prim}, but not in LR_{sem}.

Axial conductance and radial conductivity under WD

We recently described an inverse modeling approach, which allows the determination of radial and axial water transport parameters of plant roots under control and WD conditions (Boursiac et al. 2022; Bauget et al. 2023). This approach, which relies on water transport measurements in root systems that undergo successive cuts from root tip to base, allows in particular to capture the variation of radial conductance along root axis. To refine the Lp_r and anatomical analyses described above, we applied this approach to maize seedlings grown under standard conditions or under 150PEG conditions for 4 d.

In control conditions, PR and SR exhibited similar radial hydraulic conductivities (k) in the range of 2×10^{-7} m s^{-1} MPa^{-1} (Fig. 9A). Consistent with patterns of xylem differentiation, axial conductance (K) showed a gradual increase as a function of distance to root tip but was higher in PR than SR, providing a possible explanation of a higher Lp_r in the former roots. In plants grown under WD, both root types showed a 10-fold decrease in k compared with that under control conditions, in agreement with the inhibition of AQPs (Fig. 3) and enhanced suberization/lignification (Figs. 7 and 8) observed under WD conditions. The K profiles of PR and SR grown under 150PEG conditions showed a steep increase that, with respect

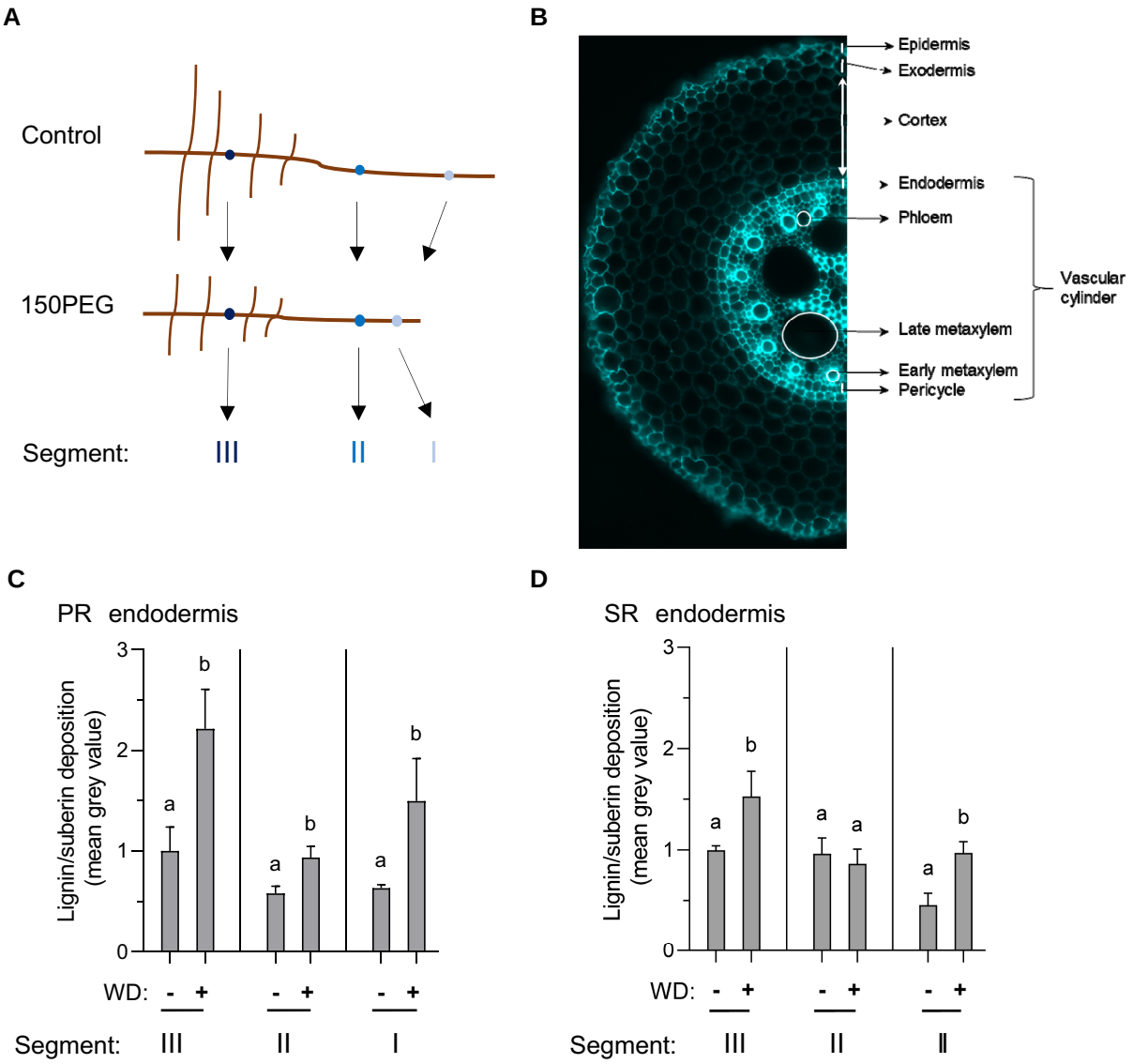

Figure 7. Deposition of suberin and lignin in PR and SR. **A)** Schematic representation of PR or SR grown in control or 150PEG conditions and separated in three segments. Segment III was the oldest one, near the root base, whereas segment I, near the root tip, was the most recently formed. **B)** Cross-section of a PR with arrows indicating the anatomical traits that were analyzed. Roots were stained with Auramine O for suberin and lignin quantification. **C, D**) Quantification of suberin/lignin in endodermis of PR (**C**) and SR (**D**). Cumulated data from two independent plant cultures (PR: $n = 12$ to 14; SR $n = 14$ to 16). Error bars indicate SEM. For each root type and segment, different letters indicate statistically different values (unpaired t test; $P < 0.05$).

to corresponding profiles under control conditions, was notably shifted to regions closer to the root tip (Fig. 9B). Nevertheless, PR and SR showed, under these WD conditions, differences in K amplitude that were comparable to those seen under control conditions. To take into account the differences in growth rate observed between root types or roots grown under control or WD, we normalized all K curves according to root age (time after sowing). These analyses revealed that PR and SR show a similar increase in K during the 5 first days, before eventually reaching distinct plateau values (Fig. 9C). Most importantly, these root specific profiles appeared to be independent of the plant growth conditions, with a reasonable overlap of all curves from 0 to 4 d. Thus, the formation and early differentiation of xylem seem to occur at a same rate in PR and SR, whether in control or WD conditions. Furthermore, the high K seen in root tips of PR and SR grown under WD (Fig. 9B) can simply be explained by their reduced growth rate, assuming that the rate of xylem differentiation indeed remains similar between control and WD conditions.

Discussion

The ability of plants to continuously adjust their water uptake capacity is based in large part on the remarkable developmental and functional plasticity of their roots. To address the integration of these phenomena, we opted to work on

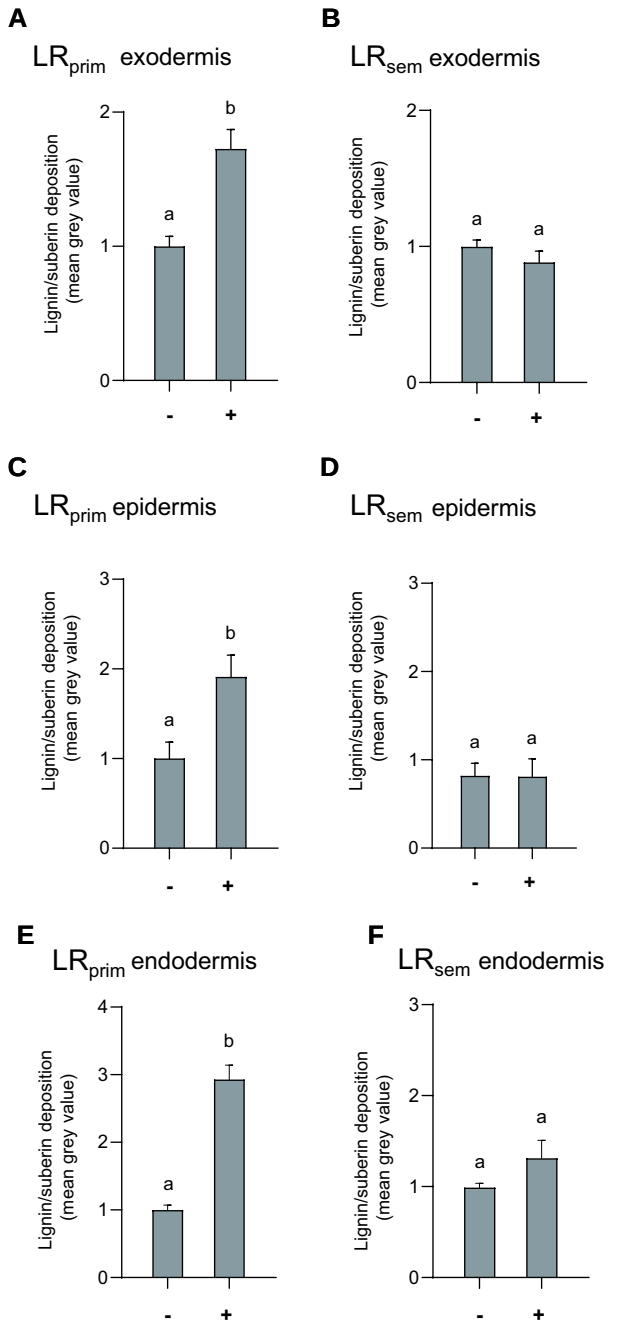

Figure 8. Deposition of suberin and lignin in LR. Plants were grown under control (WD: −) or 150PEG (WD: +) conditions and roots were stained with Auramine O for suberin and lignin quantification in the following tissues: exodermis of LR_{prim} (**A**) and LR_{sem} (**B**); epidermis of LR_{prim} (**C**) and LR_{sem} (**D**); endodermis of LR_{prim} (**E**) and LR_{sem} (**F**). Cumulated data from two independent plant cultures normalized to the LR_{prim} control. LR_{prim} control, $n = 12$; LR_{prim} 150PEG, $n = 12$; LR_{sem} control, $n = 4$; LR_{sem} 150PEG, $n = 7$. Error bars indicate SE. For each root type, different letters indicate statistically different values (Unpaired t test; $P < 0.05$).

the maize embryonic root system of a representative hybrid line (B73H). We analyzed the developmental and hydraulic properties of its different root types, under both water replete and WD conditions, thereby providing a comprehensive view of root hydraulic architecture of maize seedlings. We considered separately PR or SR systems, each comprising an axial root and its proper LR. We noted that although SR emerged at about 1 d after the PR, they maintained a growth rate that was 1.5 times lower than the one of PR, in both control and WD conditions (Fig. 1B). In addition, the PR and SR showed distinct anatomical characteristics (e.g. root diameter, number of metaxylem vessels) that remained constant throughout the 11-d-long experiments (Supplementary Fig. S7). Thus, SR are not just younger PR, as further supported by the distinct molecular (transcriptomic) profiles observed between the two root types (Tai et al. 2016).

One important finding of this work was the distinctive sensitivity of PR and SR to water availability. Under a very mild WD (50PEG; −0.070 MPa), PR maintained their axial growth, but showed a partial inhibition of LR_{prim} growth while their Lp_r was not significantly affected (Figs. 1, A, B, D and 2A). By contrast, SR showed an inhibition of axial root growth while maintaining the growth of their LR_{sem} (Fig. 1, A, C, and E) and their Lp_r was inhibited by almost half with respect to control conditions (Fig. 2B). A more pronounced, though moderate WD (150PEG; −0.33 MPa) resulted in a marked inhibition of all analyzed growth and hydraulic parameters in both PR and SR (Figs. 1 and 2). Yet, LR growth was the most impacted trait of PR, whereas this was axial root growth in SR. We speculate that, although revealed in a hydroponic system, these distinctive behaviors of PR and SR underlie integrated water uptake strategies in soil. Thus, when WD arises, as mimicked by the 50PEG treatment, PR would favor axial growth to penetrate deeper soil layers and forage for residual water thanks to their high-water transport capacity (Lp_r). This strategy is reminiscent of that of other cereals with a strong pivotal root growth such as pearl millet (*Pennisetum glaucum*) (Passot et al. 2016). Conversely, SR would restrict deep soil exploration and maintain LR growth to capture residual water in upper soil layers. When the whole soil becomes dryer, as illustrated by the 150PEG treatment, the plant would develop a conservative strategy by downregulating the growth and hydraulics of all root types. We note that dose-dependent and root-type-specific responses to WD have already been described in maize. For instance, distinct LR growth responses of PR and SR to WD were observed in two maize inbred lines (Dowd et al. 2019, 2020). These responses can vary according to genotypes as the length of LR_{prim} in one of these lines (FR697) showed, at variance with the other line (B73) or the presently studied hybrid (B73H), a bell-shaped dose response to WD and was slightly enhanced under mild WD (Dowd et al. 2019, 2020). In these and our study, most of the acclimation response of RSA to a moderate WD can be attributed to changes in axial root or LR growth and not LR formation indicating that soil exploration can rapidly resume when growth conditions are more favorable.

Whereas RSA reflects the long-term integration of elementary, water potential-dependent growth and developmental processes, we further explored the acclimation capacity of

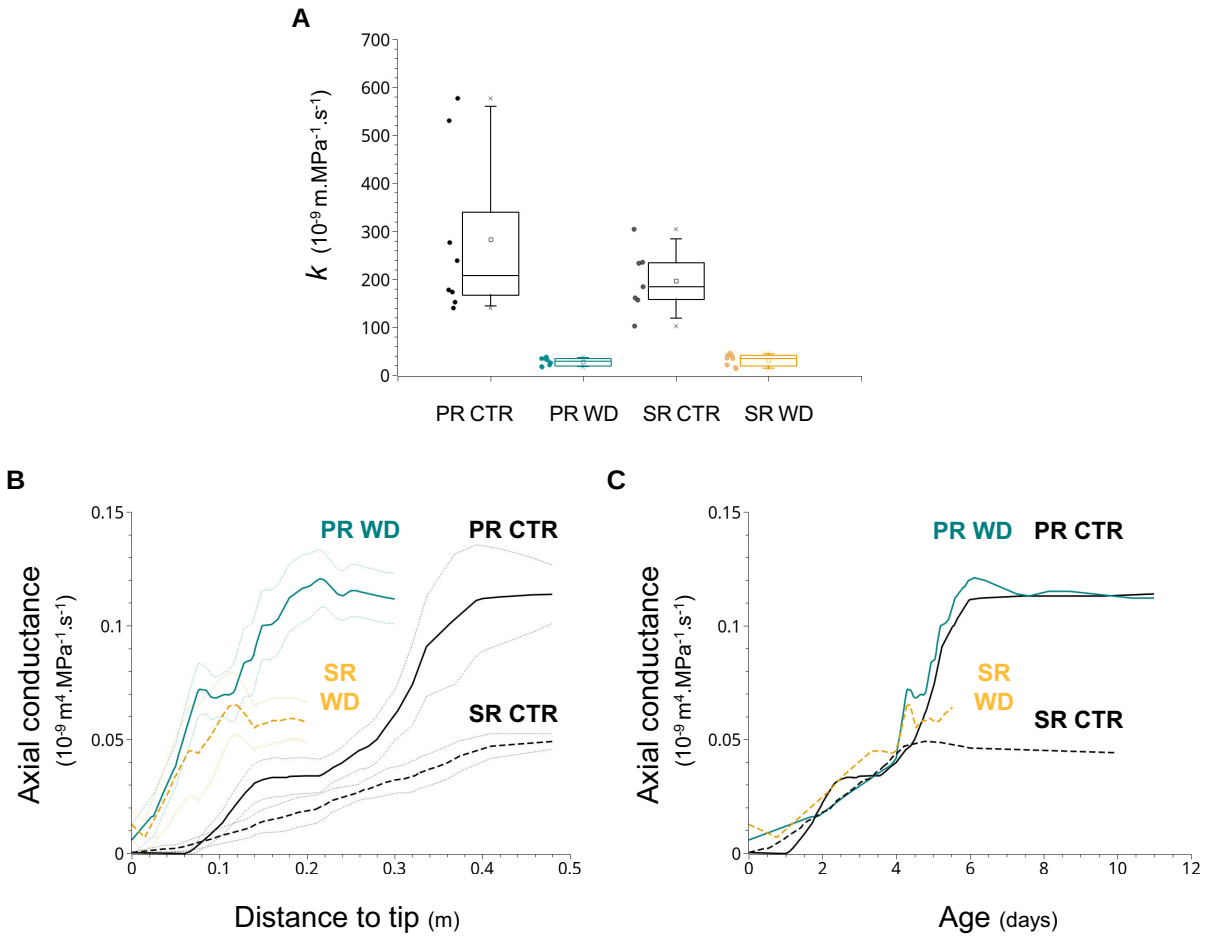

Figure 9. Model-derived hydraulic parameters of PR and SR under WD. **A)** Radial hydraulic conductivity (k) of PR and SR of plants grown in control (CTR) and 150PEG (WD) conditions. Each box indicates the 25th and 75th percentiles, while the line inside indicates the median value, and the T bars mark the 5th and 95th percentiles. The "x" and open square correspond to the extreme values and the means, respectively. **B)** Variations of axial conductance (K) as a function of distance to root tip. The solid lines represent lowest fits done on K profiles of CTR PR (black; $n = 8$), WD PR (blue; $n = 8$), CTR SR (dashed black; $n = 7$) and WD SR (orange, $n = 8$). The dot lines delineate the corresponding 95% confidence intervals. **C)** Variations of axial conductance (K) as a function of time after sowing (root age). The figure represents the same data (with same conventions) as in (**B**).

different root types using short-term kinetic experiments (Fig. 4). Notably, WD treatments resulted in a prompt (<1 h) decrease in Lp_r of both PR and SR. Conversely, the sudden release of a long-term WD was followed by a nearly as rapid recovery of Lp_r that was partial for PR and total for SR (Fig. 4). With respect to reports in other species (Tyerman et al. 1989; Boursiac et al. 2005; di Pietro et al. 2013; Kaneko et al. 2015), these measurements reveal a remarkable responsiveness of maize root hydraulics to WD. More generally, they indicate how root hydraulics provides a highly flexible means for adjusting the plant water uptake capacity, over time or during root growth across soil environments with heterogeneous water availability. This capacity may be particularly relevant for those root types such as SR that forage in upper soil layers, to capture punctual water supply resulting from rainfall or irrigation. Thus, our study highlights the importance of the maize embryonic root system in plant adaptation to WD. Thanks to its quickly adjusted and tailored responses, this root system allows for both superficial and deep soil exploration, thereby shaping the capacity of seedlings to face various drought scenarios, and enabling the plant to adapt to WD situations that would otherwise prove fatal. Given the current scenarios of climate change, which results in more frequent and earlier drought events, it is advisable to exploit the high genetic variation of maize root systems (Rishmawi et al. 2023) to select genotypes that exhibit adaptability to alternating patterns of drought and rainfall, especially during their seedling stage. To meet this criterion, the chosen genotypes should have a rapid PR growth in deeper soil layers, and a high number of SRs carrying numerous LRs, thereby boosting their plasticity. A similar idea may not apply to adult plants under prolonged drought since previous studies have shown that the growth of shoot-born roots seems to be detrimental to drought tolerance in maize and other cereals (Sanchez et al. 2002; Gao and Lynch 2016; Sebastian et al. 2016).

In order to have a more complete understanding of root type-specific functionalization and physiological responses

to WD, we also investigated the molecular and cellular mechanisms underlying maize root hydraulics.

The implication of AQPs was first probed using sodium azide, a commonly used blocker in maize and other plant species (Zhang and Tyerman 1991; Sutka et al. 2011; Rishmawi et al. 2023). In control conditions, AQP were found to contribute to more than 50% of PR and SR Lp_r and a 150PEG treatment induced a complete inhibition of AQP activity in SR whereas a residual AQP activity was observed in PR (Fig. 3). Although AQP function can be regulated at multiple levels, from transcription to aquaporin trafficking and gating (Aroca et al. 2012; Maurel et al. 2021), we restrained our study to regulation of gene expression in the whole PIP subfamily and investigated the mRNA abundance of 13 *ZmPIP* isoforms. This study, which cannot inform on aquaporin abundance nor activity, can nevertheless provide some hints at regulations at work in maize roots. Under normal conditions for instance (Fig. 2), *ZmPIP* mRNA abundance was higher in PR than SR, possibly explaining the slightly higher Lp_r of the former root type. Under both short- and long-term WD treatments, a general reduction in *ZmPIP* mRNA abundance was observed in PR, which could contribute to the WD-induced Lp_r inhibition. By contrast, WD-induced reduction of *ZmPIP* mRNA was somehow restricted to the unbranched zone of SR (Fig. 5). We speculate that the stability of *ZmPIP* mRNA abundance in LR_{sem} may allow fully reversible adjustments of AQP functions under changing water availability, thereby contributing to the high functional plasticity of SR and its laterals. At variance with WD treatments, WD removal and subsequent Lp_r increase were not associated with any change in *ZmPIP* mRNA abundance (Fig. 6). Typically, post-transcriptional and post-translational regulatory mechanisms, involving reversible PIP phosphorylation and trafficking to the plasma membrane need to be invoked in the two latter cases. Although *Zm*PIP2;5 is a main contributor of maize Lp_r, it will also be needed to dissect isoform-specific regulations to comprehend the complexity of molecular and cellular processes occurring in the maize root under WD (Hachez et al. 2006; Ding et al. 2020).

In complement to AQP expression and regulation, we also investigated possible links between WD-dependent changes in root anatomy and Lp_r (Zimmermann and Steudle 1998). In particular, the enhanced suberization/lignification of the epi- and exodermis observed under stress conditions is thought to reduce the root radial conductivity (and Lp_r) (Ranathunge and Schreiber 2011; Calvo-Polanco et al. 2021). These changes were particularly pronounced in LR_{prim} (Fig. 7A). Together with the thickening of the cortex in both LR_{prim} and axial root tip, they create mechanical barriers that hinder the total recovery of Lp_r (Wang et al. 2019; Calvo-Polanco et al. 2021). On the contrary, WD did not induce any change of suberization/lignification in LR_{sem} (Fig. 8, B to E), thereby supporting the more plastic response of SR compared to PR. Altogether, our analyses reveal a distinct developmental plasticity of LR under WD, depending on their axial root. Such response specificity of LR depending on their axis has already been observed for macroscopic parameters, such as LR length (Dowd et al. 2019, 2020). As to the present work, we realize that the hydraulics of LR could not be specifically resolved, neither through targeted water transport assays nor inverse modeling. Thus, as indicated by studies using neutron radiography of soil-grown roots (Ahmed et al. 2016), LR hydraulics may contribute to the distinctive properties attributed to whole PR or SR systems. Furthermore, it will be important to investigate the water depletion: repellency pattern induced by soil drying at the vicinity of LR, and, overall, the capacity of LR to restore water uptake upon rewatering (Cuneo et al. 2021). These characteristics may be key to understand the root response of maize seedlings to early drought in the field.

Last but not least, axial water transport was investigated using a recently developed inverse modeling approach which, we consider more accurate than investigating xylem vessel anatomy in root cross-sections and using the Hagen–Poiseuille law to infer axial conductance (K) (Boursiac et al. 2022; Bauget et al. 2023). In the present work, K was found to be higher in PR than SR, in line with the higher Lp_r of the former root type (Fig. 9B). Most importantly, our approach revealed a sharp increase of K in root tips of SR and PR grown under WD. This phenomenon may prevent axial limitations of water transport, which are the most pronounced in distal root segments, thereby optimizing water uptake in drying soil. To further investigate the bases of this dramatic change of K in root tips, we traced back the effects of root age on K. Our data (Fig. 9C) indicate that the alteration of longitudinal growth of roots by WD is sufficient to generate a unique K profile, without invoking any effects of WD on the rate of xylem differentiation. This is at variance with the positive impact of WD on xylem development, which in eudicots is mediated through enhancement by ABA of expression of VASCULAR-RELATED NAC-DOMAIN (VND) transcription factors (Ramachandran et al. 2021; Cornelis and Hazak 2022). Although xylem development is also under the control of VND-like regulators in maize, their regulation under drought might vary from what was observed in dicots (Dong et al. 2020). In addition, the thickening (increase in cell cortex size) of root tips in PR and SR axial roots and their LR also results from WD-dependent longitudinal growth arrest and has been associated to long-term effects of strong WD on root ramification (Ji et al. 2014). These examples illustrate the multiple interactions between growth and hydraulics in cereal roots under WD.

In conclusion, recent studies have revealed a dramatic natural variation of maize root hydraulic architecture pointing to various water uptake strategies within this species (Koehler et al. 2023; Rishmawi et al. 2023). Here, we investigated the response of this integrated trait to various WD, focusing on the role of embryonic roots in a typical hybrid genotype.

We propose that differences between root types in anatomical and molecular responses to WD may support their distinct functionalization and contribute to integrative acclimation responses of whole root systems to WD. Vertical

gradients of soil water availability may shape the specialization of distinct embryonic root types in order to optimize water uptake in normal and WD conditions of different intensities. By focusing on mild to moderate WD, our work emphasizes the important role of SR systems during seedling establishment. LR, which were shown to be the preferential site of water absorption in soils, would deserve more targeted investigation as they may explain the distinctive properties of their axial roots (Ahmed et al. 2016). It will also be interesting to investigate the responses to more dramatic WD conditions of adult plants with fully differentiated root systems including crown roots (Ahmed et al. 2018). Overall, the present work shows the power of combining precise anatomical, architectural, functional, and modeling studies to address the functioning of complex root systems.

Materials and methods

Plant material and growth conditions

Seeds of a maize (*Z. mays*) B73-UH007 hybrid (B73H) (Millet et al. 2016) were surface-sterilized in 1.4% (v/v) bleach, 1‰ (v/v) Tween-20, for 15 min under gentle agitation. The seeds were then treated with H_2O_2 (35%; v/v) for 2 min, rinsed with 70% (v/v) ethanol, and washed six times with sterilized water. The seeds were overlaid with wet clay beads in a plastic box, which was itself covered by a transparent plastic film. Seeds were germinated and further grown in a growth chamber at 65% relative humidity, with 15 h/9 h light/dark cycles (150 µE m^{-2} s^{-1}) at 22 °C (light)/20 °C (dark).

At 5 DAS, seedlings were transferred to hydroponic containers (61.6 × 35.8 × 13.6 cm^3; 20 seedlings/container) filled with 24 L of a medium containing 1.25 mM KNO_3, 0.75 mM $MgSO_4$, 1.5 mM $Ca(NO_3)_2$, 0.5 mM KH_2PO_4, 0.1 mM $MgCl_2$, 0.05 mM Fe-EDTA, 0.05 mM H_3BO_3, 0.012 mM $MnSO_4$, 0.7 mM $CuSO_4$, 0.001 mM $ZnSO_4$, 24×10^{-5}mM MoO_4Na_2, 1×10^{-5} mM $CoCl_2$, 0.1 mM Na_2SiO_3, and 1 mM MES. Plants were grown in this solution for 2 d. At 7 DAS, seedlings were transferred for four additional days to a fresh medium containing different concentrations of high molecular weight polyethylene glycol (PEG-8000) to reduce the water potential of the nutrient solution. This plant culture procedure makes it possible to impose WD treatments, prior to gently excising roots, and analysing both their RSA and water transport capacity. WD treatments were imposed by adding to the control solution (water potential of −0.034 MPa) 25, 50, 75, 150, or 225 g L^{-1} PEG, yielding final water potentials of −0.047, −0.070, −0,103, −0.332 or −0.700 MPa, respectively. To avoid anoxia, culture solutions were constantly bubbled with air. Solution water potential was measured with a WESCOR 5520 vapor pressure osmometer.

Analysis of RSA

Root systems were excised at 11 DAS from hydroponically grown plants and immediately imaged. PR and SR were analyzed separately. Each axial root system was manually separated on a 240 × 240 mm^2 Petri dish containing water, and scanned with an Epson Perfection V850 Pro scanner (Epson Europe BV). RSA was analyzed using the OPTIMAS image analysis software (Adept Turnkey Pty Ltd.) and ImageJ-win64. Several parameters were measured: axial root length, average length of LR, number of LR, length of non-branching zone. Total root length was quantified on the whole-root system.

Measurement of Lp_r

Measurements of Lp_r were performed using the pressure chamber technique, essentially as described by Rishmawi et al. (2023) and Bauget et al. (2023). This approach allows probing root hydraulics under control and WD conditions, taking into account both hydrostatic and osmotic forces and measuring substantial outgoing sap flows in both control and WD conditions (Bauget et al. 2023). PR and SR were excised from a same plant and analyzed separately. Upon excision, each axial root was inserted into a pressure chamber filled with the same medium as used for plant culture. For control growth conditions, the flow of exuded sap (J_v) was successively measured at pressures (P) of 50, 150, 100, 200 and 5 kPa for about 5 min at each pressure step. In 150PEG growth conditions, pressure clamps were realized at 150, 250, 200, 300 and 100 kPa in order to possibly counteract osmotically induced water efflux from the root. In either control or PEG conditions, a linear $J_v(P)$ relationship was observed in the indicated P ranges, the slope of the curve providing a correct estimate of Lp_r (Bauget et al. 2023). In kinetic experiments, J_v was first measured in the initial plant growth solution. The root was then moved into either a control solution or a solution containing 150 g L^{-1} PEG and J_v was monitored at four kinetic points (0, 20, 40, 60 min) following the same pressure protocol as above.

Root dry weight (DWr) was analyzed after measurement of J_v. The Lp_r (mL g^{-1} h^{-1} MPa^{-1}) of an individual root system was calculated using the following equation:

$$Lp_r = J_v = /(DW_r \cdot P)$$

For azide inhibition experiments, roots were exposed to a culture solution containing 1 mM NaN_3 and Lp_r was derived from continuous J_v measurement at 320 kPa as described in Sutka et al. (2011).

Total RNA isolation and analysis

Root samples were frozen in liquid nitrogen and ground by hand with pestle and mortar. Total RNA was extracted using a Direct-zol RNA Miniprep Plus kit according to the manufacturer's instructions (Zymo Research) with a modification for DNA removal with addition of five units RQ1 RNase-Free DNase (Promega) and 1 µL of a RQ1 buffer. One microgram of total RNA was used as a template for first strand complementary DNA (cDNA) synthesis, which was performed using Moloney Murine Leukemia Virus Reverse Transcriptase, RNase H Minus, Point Mutant (Promega)

and Oligo(dT)15 Primer (Promega) in a final volume of 20 μL, according to the manufacturer's instructions.

First strand cDNA was diluted 10 times, and 4 μL of cDNA were used as a template for gene expression level quantification by quantitative PCR. The latter was performed in 384-well plates with a LightCycler 480 Real-Time PCR System (Hoffmann-La Roche AG). Differentially labeled nucleotides SYBR Premix Ex Taq OneGreen Fast QPCR (ThermoFisher) were used to monitor cDNA amplification. The PCR cycle program was one cycle of predenaturation for 3 min at 95 °C for DNA polymerase activation, and 40 cycles of 5 s at 95 °C and 60 s at 60 °C. The $2^{-\Delta Ct}$ method was used to analyse the relative expression of six *ZmPIP1* (*ZmPIP1;1-ZmPIP1;6*) and six *ZmPIP2* (*ZmPIP2;1-ZmPIP2;6*) genes. The *ZmPIP2;7* gene which does not show detectable expression in the PR was not taken into account (Aroca et al. 2005; Zhu et al. 2005; Hachez et al. 2006). Two reference genes, *β-ACTIN 2* (*ACT2*) and *POLYUBIQUITIN* (*UBQ*), were used to normalize the expression (Lin et al. 2014; Ding et al. 2020). The primer sequences used for these studies are shown in Supplementary Table S1.

Auramine O staining for lignin and suberin

Root samples were collected at 11 DAS in plants grown for 4 d in the presence or absence of PEG. Excised root systems were fixed with 4% (v/v) paraformaldehyde (Merck) in 1 × PBS by vacuum infiltration for 1 h and gentle agitation at room temperature for an additional h. The fixed tissues were then washed two times for 1 min in 1 × PBS. Seedlings were then transferred into a ClearSee solution (see below) and incubated at room temperature with gentle agitation for 5 d. The solution was changed every second day. The ClearSee solution is an aqueous solution composed of 10% (w/v) xylitol, 15% (w/v) sodium deoxycholate, and 25% (w/v) urea all from Sigma. The 0.5% (w/v) Auramine O solution was directly prepared in ClearSee. Staining was performed during 12 to 16 h, followed by two washings in ClearSee during 30 min, and at least 1 h, respectively. One centimeter-long root segments were cut in the area of interest, using a Vibratome (thickness: 100 μm), and embedded in 4% (w/v) agarose. The sections were mounted on slides with ClearSee solution for imaging. Auramine O staining was imaged using a Zeiss Apotom microscope, with excitation at 488 nm and detection at 505 to 530 nm. Images were analyzed with an ImageJ-win64 software.

Determination of root axial conductance and radial conductivity by inverse modeling

The root hydraulic parameters (radial conductivity: k, m s^{-1} MPa^{-1}; axial conductance: K, m^4 s^{-1} MPa^{-1}) were determined using the HydroRoot model as described by Bauget et al. (2023). In brief, we used the cut-and-flow approach described in (Boursiac et al. 2022), which consists of measuring J_v at a given pressure in an axial root that undergoes successive cuts from the tip. PR and SR were excised from a same plant and J_v measurements were performed in the same medium as for plant growth, the operating pressure being 200 and 300 kPa in control and 150PEG conditions, respectively. While k was assumed to be uniform all over the root, the K profile was represented as a linear piecewise function of the distance to root tip. All transport parameters included in the model (Bauget et al. 2023) were adjusted to get the best fit on both $J_v(P)$ and cut-and-flow experiments.

Statistical analyses

Statistical analysis was performed using the GraphPad Prism5. Student's *t* test and one-way ANOVA followed by a Tukey test were performed to determine significant differences between groups of samples, as indicated by different letters.

Accession numbers

Sequence data from this article can be found in the GenBank/EMBL data libraries under accession numbers (Supplementary Table S1).

Acknowledgments

We thank the PHIV imaging platform and Carine Alcon for help with the anatomical analyses.

Author contributions

V.P. and C.M. conceived the study. V.P. performed all of the experiments except for the modeling part. F.B. did the modeling experiment. L.R. assisted in running the experiments and in data analysis. P.N. provided essential advice and tools for running the experiments. V.P. and C.M. wrote the manuscript which was reviewed by all the authors.

Supplementary data

The following materials are available in the online version of this article.

Supplementary Figure S1. RSA response of PR and SR to various PEG concentrations.

Supplementary Figure S2. Growth and developmental responses of PR and SR to 50PEG and 150PEG conditions.

Supplementary Figure S3. PR and SR hydraulic and leaf growth responses to WD.

Supplementary Figure S4. Kinetic analysis of root hydraulic conductivity (Lp_r) of PR and SR in response to a sudden change in solute concentration in the bathing solution.

Supplementary Figure S5. Relative expression of representative *ZmPIP1* and *ZmPIP2* genes in the LR of PR and SR after short-term (1 h) imposition of a change in PEG concentration in the root bathing solution.

Supplementary Figure S6. Deposition of suberin and lignin in PR and SR in response to WD.

Supplementary Figure S7. Anatomic traits of PR and SR in control and WD conditions.

Supplementary Figure S8. Anatomic traits of LR_{prim} and LR_{sem} in control and WD conditions.

Supplementary Table S1. Gene accession numbers and primer sequences.

Funding

This work was supported by the European Research Council (ERC) under the European Union's Horizon 2020 research and innovation programme (Grant Agreement ERC-2017-ADG-788553).

Conflict of interest statement. None declared.

Data availability

Data supporting the findings of this study are available within the paper, within its Supplemental data published online or on request.

References

Ahmed MA, Zarebanadkouki M, Kaestner A, Carminati A. Measurements of water uptake of maize roots: the key function of lateral roots. Plant Soil. 2016:**398**(1–2):59–77. https://doi.org/10.1007/s11104-015-2639-6

Ahmed MA, Zarebanadkouki M, Meunier F, Javaux M, Kaestner A, Carminati A. Root type matters: measurement of water uptake by seminal, crown, and lateral roots in maize. J Exp Bot. 2018:**69**(5):1199–1206. https://doi.org/10.1093/jxb/erx439

Aroca R, Amodeo G, Fernández-Illescas S, Herman EM, Chaumont FO, Chrispeels MJ. The role of aquaporins and membrane damage in chilling and hydrogen peroxide induced changes in the hydraulic conductance of maize roots. Plant Physiol. 2005:**137**(1):341–353. https://doi.org/10.1104/pp.104.051045

Aroca R, Porcel R, Ruiz-Lozano JM. Regulation of root water uptake under abiotic stress conditions. J Exp Bot. 2012:**63**(1):43–57. https://doi.org/10.1093/jxb/err266

Bauget F, Protto V, Pradal C, Boursiac Y, Maurel C. A root functional-structural model allows assessment of the effects of water deficit on water and solute transport parameters. J Exp Bot. 2023:**74**(5):1594–1608. https://doi.org/10.1093/jxb/erac471

Boursiac Y, Chen S, Luu DT, Sorieul M, van den Dries N, Maurel C. Early effects of salinity on water transport in Arabidopsis roots. Molecular and cellular features of aquaporin expression. Plant Physiol. 2005:**139**(2):790–805. https://doi.org/10.1104/pp.105.065029

Boursiac Y, Protto V, Rishmawi L, Maurel C. Experimental and conceptual approaches to root water transport. Plant Soil. 2022:**478**(1–2):349–370. https://doi.org/10.1007/s11104-022-05427-z

Bray AL, Topp CN. The quantitative genetic control of root architecture in maize. Plant Cell Physiol. 2018:**59**(10):1919–1930. https://doi.org/10.1093/pcp/pcy141

Caldeira CF, Bosio M, Parent B, Jeanguenin L, Chaumont F, Tardieu F. A hydraulic model is compatible with rapid changes in leaf elongation under fluctuating evaporative demand and soil water status. Plant Physiol. 2014:**164**(4):1718–1730. https://doi.org/10.1104/pp.113.228379

Calvo-Polanco M, Ribeyre Z, Dauzat M, Reyt G, Hidalgo-Shrestha C, Diehl P, Frenger M, Simonneau T, Muller B, Salt DE, et al. Physiological roles of Casparian strips and suberin in the transport of water and solutes. New Phytol. 2021:**232**(6):2295–2307. https://doi.org/10.1111/nph.17765

Cornelis S, Hazak O. Understanding the root xylem plasticity for designing resilient crops. Plant Cell Environ. 2022:**45**(3):664–676. https://doi.org/10.1111/pce.14245

Cuneo IF, Barrios-Masias F, Knipfer T, Uretsky J, Reyes C, Lenain P, Brodersen CR, Walker MA, McElrone AJ. Differences in grapevine rootstock sensitivity and recovery from drought are linked to fine root cortical lacunae and root tip function. New Phytol. 2021:**229**(1):272–283. https://doi.org/10.1111/nph.16542

di Pietro M, Vialaret J, Li GW, Hem S, Prado K, Rossignol M, Maurel C, Santoni V. Coordinated post-translational responses of aquaporins to abiotic and nutritional stimuli in Arabidopsis roots. Mol Cell Proteomics. 2013:**12**(12):3886–3897. https://doi.org/10.1074/mcp.M113.028241

Ding L, Milhiet T, Couvreur V, Nelissen H, Meziane A, Parent B, Aesaert S, Van Lijsebettens M, Inze D, Tardieu F, et al. Modification of the expression of the aquaporin ZmPIP2; 5 affects water relations and plant growth. Plant Physiol. 2020:**182**(4):2154–2165. https://doi.org/10.1104/pp.19.01183

Dong Z, Xu Z, Xu L, Galli M, Gallavotti A, Dooner HK, Chuck G. Necrotic upper tips1 mimics heat and drought stress and encodes a protoxylem-specific transcription factor in maize. Proc Natl Acad Sci U S A. 2020:**117**(34):20908–20919. https://doi.org/10.1073/pnas.2005014117

Dowd TG, Braun DM, Sharp RE. Maize lateral root developmental plasticity induced by mild water stress. I: genotypic variation across a high-resolution series of water potentials. Plant Cell Environ. 2019:**42**(7):2259–2273. https://doi.org/10.1111/pce.13399

Dowd TG, Braun DM, Sharp RE. Maize lateral root developmental plasticity induced by mild water stress. II: genotype-specific spatio-temporal effects on determinate development. Plant Cell Environ. 2020:**43**(10):2409–2427. https://doi.org/10.1111/pce.13840

Gao Y, Lynch JP. Reduced crown root number improves water acquisition under water deficit stress in maize (Zea mays L.). J Exp Bot. 2016:**67**(15):4545–4557. https://doi.org/10.1093/jxb/erw243

Hachez C, Moshelion M, Zelazny E, Cavez D, Chaumont F. Localization and quantification of plasma membrane aquaporin expression in maize primary root: a clue to understanding their role as cellular plumbers. Plant Mol Biol. 2006:**62**(1–2):305–323. https://doi.org/10.1007/s11103-006-9022-1

Hachez C, Veselov D, Ye Q, Reinhardt H, Knipfer T, Fricke W, Chaumont F. Short-term control of maize cell and root water permeability through plasma membrane aquaporin isoforms. Plant Cell Environ. 2012:**35**(1):185–198. https://doi.org/10.1111/j.1365-3040.2011.02429.x

Hochholdinger F, Park WJ, Sauer M, Woll K. From weeds to crops: genetic analysis of root development in cereals. Trends Plant Sci. 2004a:**9**(1):42–48. https://doi.org/10.1016/j.tplants.2003.11.003

Hochholdinger F, Tuberosa R. Genetic and genomic dissection of maize root development and architecture. Curr Opin Plant Biol. 2009:**12**(2):172–177. https://doi.org/10.1016/j.pbi.2008.12.002

Hochholdinger F, Woll K, Sauer M, Dembinsky D. Genetic dissection of root formation in maize (Zea mays) reveals root-type specific developmental programmes. Ann Bot. 2004b:**93**(4):359–368. https://doi.org/10.1093/aob/mch056

Hochholdinger F, Yu P, Marcon C. Genetic control of root system development in maize. Trends Plant Sci. 2018:**23**(1):79–88. https://doi.org/10.1016/j.tplants.2017.10.004

Jackson RB, Sperry JS, Dawson TE. Root water uptake and transport: using physiological processes in global predictions. Trends Plant Sci. 2000:**5**(11):482–488. https://doi.org/10.1016/S1360-1385(00)01766-0

Javot H, Maurel C. The role of aquaporins in root water uptake. Ann Bot. 2002:**90**(3):301–313. https://doi.org/10.1093/aob/mcf199

Ji H, Liu L, Li K, Xie Q, Wang Z, Zhao X, Li X. PEG-mediated osmotic stress induces premature differentiation of the root apical meristem and outgrowth of lateral roots in wheat. J Exp Bot. 2014:**65**(17):4863–4872. https://doi.org/10.1093/jxb/eru255

Kaneko T, Horie T, Nakahara Y, Tsuji N, Shibasaka M, Katsuhara M. Dynamic regulation of the root hydraulic conductivity of barley

plants in response to salinity/osmotic stress. Plant Cell Physiol. 2015:**56**(5):875–882. https://doi.org/10.1093/pcp/pcv013

Koehler T, Schaum C, Tung SY, Steiner F, Tyborski N, Wild AJ, Akale A, Pausch J, Lueders T, Wolfrum S, et al. Above and belowground traits impacting transpiration decline during soil drying in 48 maize (Zea mays) genotypes. Ann Bot. 2023:**131**(2):373–386. https://doi.org/10.1093/aob/mcac147

Lin Y, Zhang C, Lan H, Gao S, Liu H, Liu J, Cao M, Pan G, Rong T, Zhang S. Validation of potential reference genes for qPCR in maize across abiotic stresses, hormone treatments, and tissue types. PLoS One. 2014:**9**(5):e95445. https://doi.org/10.1371/journal.pone.0095445

Lynch J. Root architecture and plant productivity. Plant Physiol. 1995:**109**(1):7–13. https://doi.org/10.1104/pp.109.1.7

Lynch JP, Chimungu JG, Brown KM. Root anatomical phenes associated with water acquisition from drying soil: targets for crop improvement. J Exp Bot. 2014:**65**(21):6155–6166. https://doi.org/10.1093/jxb/eru162

Maurel C, Boursiac Y, Luu DT, Santoni V, Shahzad Z, Verdoucq L. Aquaporins in plants. Physiol Rev. 2015:**95**(4):1321–1358. https://doi.org/10.1152/physrev.00008.2015

Maurel C, Nacry P. Root architecture and hydraulics converge for acclimation to changing water availability. Nat Plants. 2020:**6**(7):744–749. https://doi.org/10.1038/s41477-020-0684-5

Maurel C, Tournaire-Roux C, Verdoucq L, Santoni V. Hormonal and environmental signaling pathways target membrane water transport. Plant Physiol. 2021:**187**(4):2056–2070. https://doi.org/10.1093/plphys/kiab373

McCully ME. Roots in soil: unearthing the complexities of roots and their rhizospheres. Annu Rev Plant Physiol Plant Mol Biol. 1999:**50**(1):695–718. https://doi.org/10.1146/annurev.arplant.50.1.695

McCully ME, Canny MJ. Pathways and processes of water and nutrient movement in roots. Plant Soil. 1988:**111**(2):159–170. https://doi.org/10.1007/BF02139932

Millet EJ, Welcker C, Kruijer W, Negro S, Coupel-Ledru A, Nicolas SD, Laborde J, Bauland C, Praud S, Ranc N, et al. Genome-wide analysis of yield in Europe: allelic effects vary with drought and heat scenarios. Plant Physiol. 2016:**172**:749–764. https://doi.org/10.1104/pp.16.00621

Ogura T, Goeschl C, Filiault D, Mirea M, Slovak R, Wolhrab B, Satbhai SB, Busch W. Root system depth in Arabidopsis is shaped by EXOCYST70A3 via the dynamic modulation of auxin transport. Cell. 2019:**178**(2):400–412 e16. https://doi.org/10.1016/j.cell.2019.06.021

Passot S, Gnacko F, Moukouanga D, Lucas M, Guyomarc'h S, Ortega BM, Atkinson JA, Belko MN, Bennett MJ, Gantet P, et al. Characterization of pearl millet root architecture and anatomy reveals three types of lateral roots. Front Plant Sci. 2016:**7**:829. https://doi.org/10.3389/fpls.2016.00829

Ramachandran P, Augstein F, Mazumdar S, Nguyen TV, Minina EA, Melnyk CW, Carlsbecker A. Abscisic acid signaling activates distinct VND transcription factors to promote xylem differentiation in Arabidopsis. Curr Biol. 2021:**31**(14):3153–3161.e5. https://doi.org/10.1016/j.cub.2021.04.057

Ramachandran P, Wang G, Augstein F, de Vries J, Carlsbecker A. Continuous root xylem formation and vascular acclimation to water deficit involves endodermal ABA signalling via miR165. Development. 2018:**145**:dev159202. https://doi.org/10.1242/dev.159202

Ranathunge K, Schreiber L. Water and solute permeabilities of Arabidopsis roots in relation to the amount and composition of aliphatic suberin. J Exp Bot. 2011:**62**(6):1961–1974. https://doi.org/10.1093/jxb/erq389

Rishmawi L, Bauget F, Protto V, Bauland C, Nacry P, Maurel C. Natural variation of maize root hydraulic architecture underlies highly diverse water uptake capacities. Plant Physiol. 2023:**192**(3):2404–2418. https://doi.org/10.1093/plphys/kiad213

Rosales MA, Maurel C, Nacry P. Abscisic acid coordinates dose-dependent developmental and hydraulic responses of roots to water deficit. Plant Physiol. 2019:**180**(4):2198–2211. https://doi.org/10.1104/pp.18.01546

Sanchez AC, Subudhi PK, Rosenow DT, Nguyen HT. Mapping QTLs associated with drought resistance in sorghum (Sorghum bicolor L. Moench). Plant Mol Biol. 2002:**48**(5/6):713–726. https://doi.org/10.1023/A:1014894130270

Schmidhalter U, Evéquoz M, Camp K-H, Studer C. Sequence of drought response of maize seedlings in drying soil. Physiol Plant. 1998:**104**(2):159–168. https://doi.org/10.1034/j.1399-3054.1998.1040203.x

Sebastian J, Yee MC, Goudinho Viana W, Rellan-Alvarez R, Feldman M, Priest HD, Trontin C, Lee T, Jiang H, Baxter I, et al. Grasses suppress shoot-borne roots to conserve water during drought. Proc Natl Acad Sci U S A. 2016:**113**(31):8861–8866. https://doi.org/10.1073/pnas.1604021113

Seiler GJ. Influence of temperature on primary and lateral root growth of sunflower seedlings. Environ Exp Bot. 1998:**40**(2):135–146. https://doi.org/10.1016/S0098-8472(98)00027-6

Sharp RE, Davies WJ. Solute regulation and growth by roots and shoots of water-stressed maize plants. Planta. 1979:**147**(1):43–49. https://doi.org/10.1007/BF00384589

Sharp RE, Davies WJ. Root growth and water uptake by maize plants in drying soil. J Exp Bot. 1985:**36**(9):1441–1456. https://doi.org/10.1093/jxb/36.9.1441

Sharp RE, Davies WJ. Regulation of growth and development of plants growing with a restricted supply of water. In: **Jones HG, Jones MB, Flowers TJ**, editors. Plants under stress: biochemistry, physiology and ecology and their application to plant improvement. Cambridge: Cambridge University Press; 1989. p. 71–94.

Sharp RE, Poroyko V, Hejlek LG, Spollen WG, Springer GK, Bohnert HJ, Nguyen HT. Root growth maintenance during water deficits: physiology to functional genomics. J Exp Bot. 2004:**55**(407):2343–2351. https://doi.org/10.1093/jxb/erh276

Sharp RE, Silk WK, Hsiao TC. Growth of the maize primary root at low water potentials: I. spatial distribution of expansive growth. Plant Physiol. 1988:**87**(1):50–57. https://doi.org/10.1104/pp.87.1.50

Shukla V, Barberon M. Building and breaking of a barrier: suberin plasticity and function in the endodermis. Curr Opin Plant Biol. 2021:**64**:102153. https://doi.org/10.1016/j.pbi.2021.102153

Siemens JA, Zwiazek JJ. Changes in root water flow properties of solution culture-grown trembling aspen (*Populus tremuloides*) seedlings under different intensities of water-deficit stress. Physiol Plant. 2004:**121**(1):44–49. https://doi.org/10.1111/j.0031-9317.2004.00291.x

Steudle E. Water uptake by roots: effects of water deficit. J Exp Bot. 2000:**51**(350):1531–1542. https://doi.org/10.1093/jexbot/51.350.1531

Steudle E. The cohesion-tension mechanism and the acquisition of water by plant roots. Annu Rev Plant Physiol Plant Mol Biol. 2001:**52**(1):847–875. https://doi.org/10.1146/annurev.arplant.52.1.847

Sutka M, Li G, Boudet J, Boursiac Y, Doumas P, Maurel C. Natural variation of root hydraulics in Arabidopsis grown in normal and salt-stressed conditions. Plant Physiol. 2011:**155**(3):1264–1276. https://doi.org/10.1104/pp.110.163113

Tai H, Lu X, Opitz N, Marcon C, Paschold A, Lithio A, Nettleton D, Hochholdinger F. Transcriptomic and anatomical complexity of primary, seminal, and crown roots highlight root type-specific functional diversity in maize (Zea mays L.). J Exp Bot. 2016:**67**(4):1123–1135. https://doi.org/10.1093/jxb/erv513

Tang N, Shahzad Z, Lonjon F, Loudet O, Vailleau F, Maurel C. Natural variation at XND1 impacts root hydraulics and trade-off for stress responses in Arabidopsis. Nat Commun. 2018:**9**(1):3884. https://doi.org/10.1038/s41467-018-06430-8

Tyerman S, Oats P, Gibbs J, Dracup M, Greenway H. Turgor-volume regulation and cellular water relations of *Nicotiana tabacum* roots grown in high salinities. Funct Plant Biol. 1989:**16**(6):517–531. https://doi.org/10.1071/PP9890517

Van der Weele CM, Spollen WG, Sharp RE, Baskin TI. Growth of *Arabidopsis thaliana* seedlings under water deficit studied by control

of water potential in nutrient-agar media. J Exp Bot. 2000:**51**(350): 1555–1562. https://doi.org/10.1093/jexbot/51.350.1555

Vandeleur RK, Mayo G, Shelden MC, Gilliham M, Kaiser BN, Tyerman SD. The role of plasma membrane intrinsic protein aquaporins in water transport through roots: diurnal and drought stress responses reveal different strategies between isohydric and anisohydric cultivars of grapevine. Plant Physiol. 2009:**149**(1):445–460. https://doi.org/10.1104/pp.108.128645

Wang P, Calvo-Polanco M, Reyt G, Barberon M, Champeyroux C, Santoni V, Maurel C, Franke RB, Ljung K, Novak O, et al. Surveillance of cell wall diffusion barrier integrity modulates water and solute transport in plants. Sci Rep. 2019:**9**(1):4227. https://doi.org/10.1038/s41598-019-40588-5

Zhan A, Schneider H, Lynch JP. Reduced lateral root branching density improves drought tolerance in maize. Plant Physiol. 2015:**168**(4): 1603–1615. https://doi.org/10.1104/pp.15.00187

Zhang W, Tyerman S. Effect of low O_2 concentration and azide on hydraulic conductivity and osmotic volume of the cortical cells of wheat roots. Funct Plant Biol. 1991:**18**(6):603–613. https://doi.org/10.1071/PP9910603

Zhu C, Schraut D, Hartung W, Schaffner AR. Differential responses of maize MIP genes to salt stress and ABA. J Exp Bot. 2005:**56**(421): 2971–2981. https://doi.org/10.1093/jxb/eri294

Zimmermann HM, Steudle E. Apoplastic transport across young maize roots: effect of the exodermis. Planta. 1998:**206**(1):7–19. https://doi.org/10.1007/s004250050368